

Simplified modelling of continuous buried pipelines subject to earthquake fault rupture

Roberto Paolucci*¹, Stefano Griffini², Stefano Mariani¹

¹*Department of Structural Engineering, Politecnico di Milano, P.zza Leonardo da Vinci 32, 20133 Milano, Italy*

²*SOIL srl, v. Pestalozzi 10, Milano, Italy*

(Received March 30, 2010, Accepted July 14, 2010)

Abstract. A novel simple approach is presented for the seismic analysis of continuous buried pipelines subject to fault ruptures. The method is based on the minimization of the total dissipated energy during faulting, taking into account the basic factors that affect the problem, namely: a) the pipe yielding under axial and bending load, through the formation of plastic hinges and axial slip; b) the longitudinal friction across the pipe-soil interface; c) the lateral resistance of soil. The advantages and drawbacks of the proposed method are highlighted through a comparison with previous approaches, as well as with finite element calculations accounting for the 3D kinematics of the pipe-soil-fault systems under large deformations. Parametric analyses are also provided to assess the relative influence of the various parameters affecting the problem.

Keywords: buried pipeline; fault rupture; seismic design; finite element simulations.

1. Introduction

The seismic analysis of buried pipelines crossing active faults is a difficult task, involving a complicated soil-structure interaction problem with several major numerical difficulties, such as: i) 3D geometry; ii) large deformations; iii) local cross-sectional buckling; iv) Eulerian buckling under compressive fault movement; v) pipe sliding with respect to the surrounding soil; vi) non-linear soil behaviour. Furthermore, unless the fault breakage occurs within a narrow zone, as for relatively rigid ground materials, the longitudinal extension of the pipe affected by large deformations may reach in some cases several tens of meters.

A well documented example of a large water transmission pipeline subject to the strike-slip fault-rupture of the August 17, 1999, M_w 7.5 Kocaeli earthquake, that devastated Western Turkey, is reported by Eidingner *et al.* (2002). The pipe had a thin-walled circular cross-section with external diameter $D = 2.2$ m and thickness $t = 18$ mm. In that case, the primary pipe deformation zone, due to a fault offset of about 3 m, was around 30 m long, with two major wrinkles occurring within this zone at a relative distance of about 17 m, causing significant leakage and partial tear. A sketch of the pipeline damage is reported in Fig. 1.

As in the Turkish case, damage to buried pipelines in the presence of surface fault ruptures has been frequently observed during major earthquakes (see e.g. O'Rourke and Palmer 1996, Oka 1996,

* Corresponding author, Professor, E-mail: paolucci@stru.polimi.it

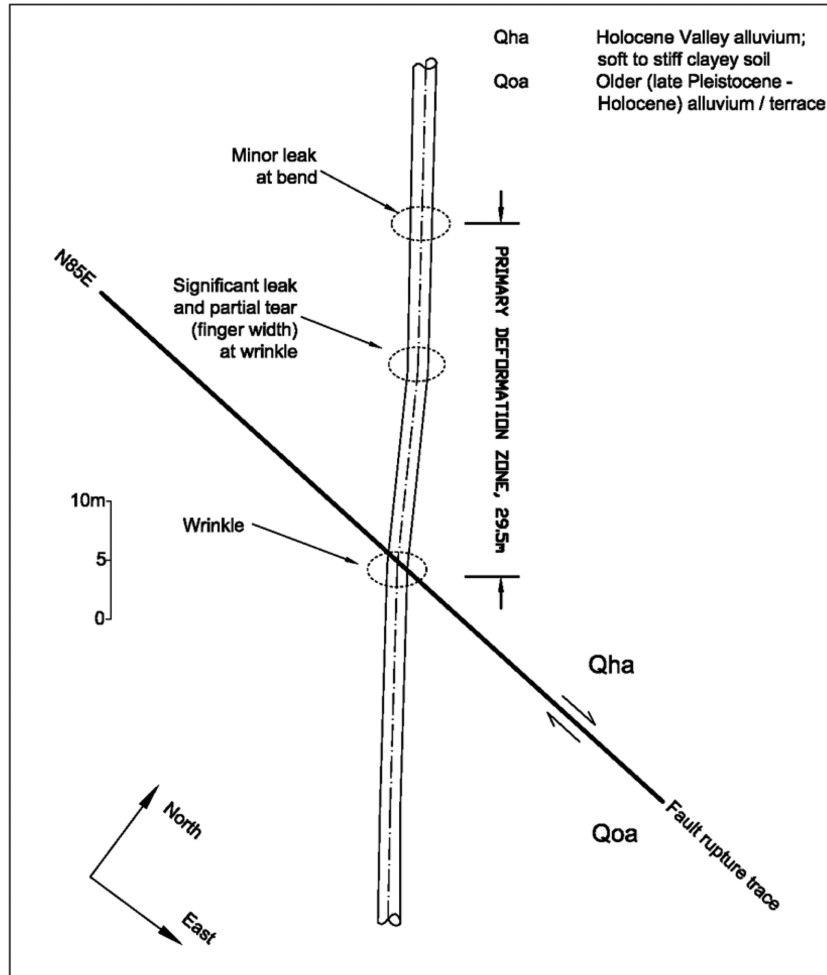


Fig. 1 Water transmission pipeline damage during the Kocaeli 1999 Turkey earthquake. Adapted from Eidinger *et al.* (2002)

Miyajima and Hashimoto 2001). However, even under a moderate magnitude seismic event, such as the April 6, 2009, M_w 6.3 L'Aquila, Central Italy, a major water transmission steel pipeline, with 60 cm diameter, underwent a local failure as a consequence of a 15 cm normal fault offset, crossing the pipe transverse to its longitudinal axis.

This growing set of observations has led to improved knowledge about interaction of the fault rupture with the buried pipe and to the introduction of updated vulnerability functions (see e.g. O'Rourke and Deyoe 2004, Pineda-Porras and Najafi 2010), although well documented case-histories and experimental results are still relatively few to calibrate numerical approaches (see e.g. Ha *et al.* 2008).

Numerical simulations of such problem may be very difficult, even with suitable finite element (FE) approaches (Takada *et al.* 2001, Liu *et al.* 2004, Ogawa *et al.* 2004, Guo *et al.* 2004), that clearly highlighted the role of large flexural strain localization and local buckling occurring at few cross-sections along the pipe, the remaining parts being nearly unaffected.

Most of the available engineering approaches to tackle this problem stem from the pioneering work of Newmark and Hall (1975), who devised a simple method whereby the pipe was modelled as a cable, connected to the soil by nonlinear springs, and elongating in the axial direction within a finite region, the extension of which was determined based on geometrical and material compatibility conditions. The Newmark and Hall approach was subsequently improved by Kennedy *et al.* (1977) to take simply into account the flexural deformation of the pipe and the transversal soil resistance as well.

Drawbacks of the previous engineering approaches were highlighted by Wang and Yeh (1985) and, more recently, by Karamitros *et al.* (2007). The latter authors devised an approximate solution that exploits the beam-on-elastic-foundation theory coupled with the classic solutions for a beam cross-section under axial load and bending to find out the pipeline cross-sections subject to the most unfavourable combination of loading.

A novel simple approach is proposed in this paper limited in this application to strike-slip faults, but easily extendible to other fault types. This approach, based on energy considerations, may be helpful for overcoming some of the drawbacks of the available engineering approaches. As a matter of fact, on one side, it allows consideration of both tensile and compression conditions on the pipe, and, on the other side, it allows one to take into account in an approximate way the loss of flexural stiffness of the pipe in few selected cross-sections.

After presentation of the method, based on the minimization of the power required to lead the structure to a prescribed limit state, several comparisons are shown, both with previous simplified approaches and with advanced 3D finite element analyses, where both the soil and the pipe are modelled by nonlinear solid (brick) elements, suitable frictional soil-pipe interaction and finite strain kinematics of the pipe-soil-fault system are considered.

Based on the previous comparisons, the results of the proposed simplified approach are critically reviewed, and then applied for a parametric analysis where the effect of the fault-intersection angle, of the soil-pipe friction angle, of the embedment depth and of the cross-sectional thickness of the pipe are illustrated and assessed according to the Eurocode 8 prescriptions, involving performance-design criteria based on maximum pipe strains. Therefore, the proposed approach, and the 3D numerical finite element approach proposed for its validation, will not be tested against collapse limit states involving the onset of buckling in the thin-walled cross-sections (e.g. Houliara and Karamanos 2006), that is beyond its scope and capability.

2. Method

In the proposed method, a failure mechanism for the pipe is assumed, consisting of two plastic hinges at both sides of the pipe relative to the fault trace, where the flexural deformation of the pipe is assumed to be concentrated. In the simplest case, i.e. strike-slip fault with homogeneous ground conditions, the plastic hinges are anti-symmetric with respect to the fault-pipe crossing. In the region within the two plastic hinges, the pipe elongates (or shrinks) plastically. Due to the complex 3D nature of the problem, it would be practically unfeasible to devise a corresponding failure mechanism for the surrounding soil, in order to introduce the method in the theoretical framework of the kinematic approach to plastic collapse. Rather, the soil-structure interaction is taken into account with the assumption that the pipe movement is constrained, both in the axial and transverse direction, by a distribution of forces determined according to empirical formulas available from the

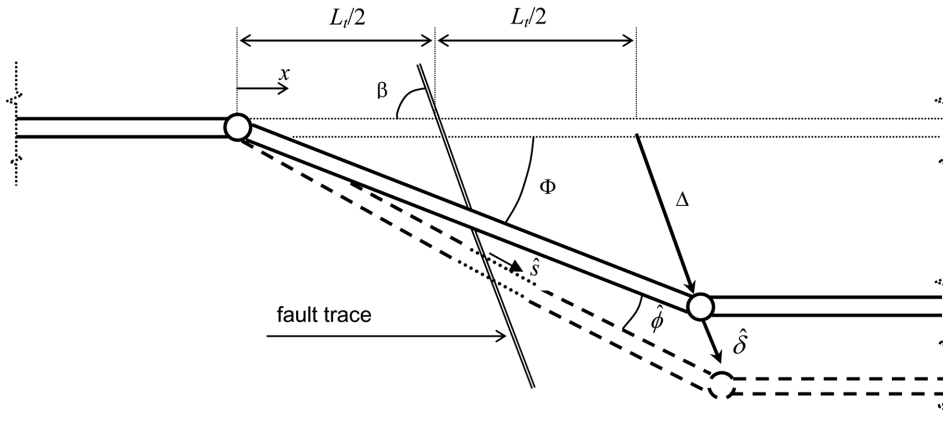


Fig. 2 Assumed failure mechanism for the continuous pipeline crossed by a strike-slip fault

literature. A comprehensive review of such formulas can be found in O'Rourke and Liu (1999) and several examples of practical applications in ALA (2001).

The sketch of the proposed failure mechanism for the pipe is shown in Fig. 2. Although this figure, as well as the following examples for validation and application, are based on the strike-slip fault and homogeneous soil assumptions, so that symmetry considerations are feasible, the approach can easily be extended to account for normal and reverse fault movement, and inhomogeneous soil conditions as well.

The single geometrical unknown of the failure mechanism is the angle Φ formed by the pipe axis with respect to the original one, corresponding to a prescribed fault displacement Δ . To obtain this unknown, the system is subjected to an infinitesimal (virtual) increment of fault displacement $\hat{\delta}$ (see Fig. 2). The resisting power P_r dissipated by the different forces acting on the system is calculated as the sum of four contributions

$$P_r = P_{r1} + P_{r2} + P_{r3} + P_{r4} \quad (1)$$

where the various terms in Eq. (1) are calculated as follows.

$$\text{Plastic hinges:} \quad P_{r1} = 2M_p \hat{\phi} \quad (2)$$

where

$$M_p = \frac{4}{3} \sigma_y (R_e^3 - R_i^3) \quad (3)$$

is the plastic moment of a hollow circular pipe cross-section when the plastic resources of the material are fully mobilized, R_e and R_i being the external and internal cross-sectional radius, respectively, and σ_y the yield stress of the material. Furthermore, based on simple geometrical relationships

$$\hat{\phi} = \hat{\delta} \frac{\sin \Phi \sin(\beta - \Phi)}{\Delta \sin \beta} \quad (4)$$

is the infinitesimal increment of rotation across the hinge, due to the infinitesimal fault displacement

increment $\hat{\delta}$.

Plastic elongation of the pipe $P_{r2} = F_p \cdot \hat{s}$ (5)

where

$$F_p = \pi \sigma_y (R_e^2 - R_i^2) \quad (6)$$

is the axial force corresponding to the full mobilization of the cross-sectional plastic resources, and

$$\hat{s} = \hat{\delta} \cos(\beta - \Phi) \quad (7)$$

is the infinitesimal elongation (or shrinkage) of the pipe trunk between the two hinges.

Longitudinal sliding $P_{r3} = \int_0^{L_t} t_u(x) \hat{s}(x) dx$ (8)

where t_u is the limit resisting force per unit length at the pipe-soil interface in the longitudinal direction, due to relative sliding of the pipe with respect to the surrounding soil. For homogeneous soil conditions t_u does not depend on x . Typical expressions of t_u for both cohesionless and cohesive soils can be found in ALA (2001). Furthermore

$$\hat{s}(x) = \hat{\delta} \frac{\sin \Phi \cos(\beta - \Phi)}{\Delta \sin \beta} x \quad (9)$$

is the pipe elongation at distance x from the left plastic hinge, while

$$L_t = \Delta \frac{\sin \beta}{\sin \Phi} \quad (10)$$

is the length of the pipe trunk between the two hinges.

Horizontal transverse movement $P_{r4} = \int_0^{L_t} p_u(x) \hat{\delta}_t(x) dx$ (11)

where p_u is the limit resisting force per unit length transmitted to the pipe, due to the pipe movement in the transverse direction. As for t_u , for typical expressions of p_u the reader is referred to ALA (2001). The transverse component of displacement is given by

$$\hat{\delta}_t(x) = \hat{\delta} \frac{x}{\Delta} \sin \Phi \quad (12)$$

The system configuration corresponding to the full mobilization of the soil and structural strength is obtained by minimizing the resisting power (1) with respect to the unknown parameter Φ , whence, by a simple geometric relationship, the unknown distance between the two plastic hinges can be found. A sample plot of P_r is shown in Fig. 3, where the white thick line highlights, for each imposed displacement Δ , the Φ value that minimizes P_r . The model parameters are the same as in the example illustrated in section 3.2. The corresponding failure mechanisms for different imposed fault offsets in the case $\beta = 90^\circ$, i.e. strike-slip direction orthogonal to the pipe axis, are shown in Fig. 4.

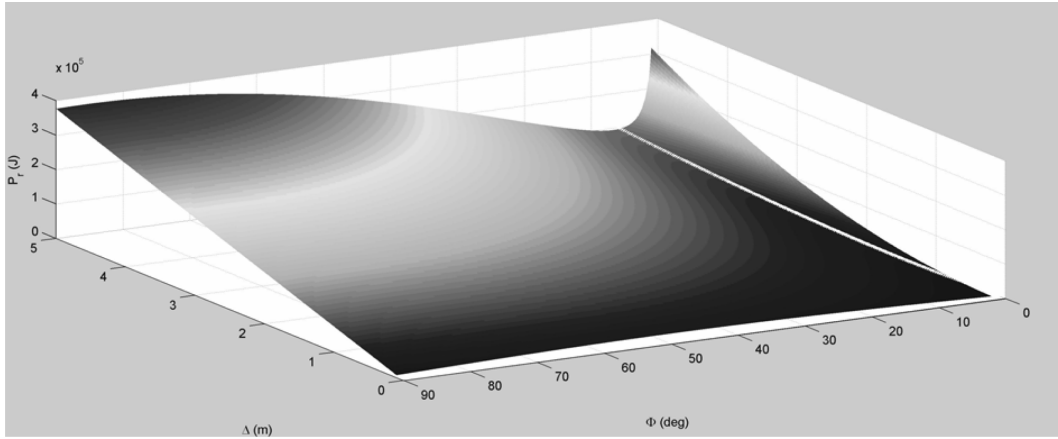


Fig. 3 Plot of the resisting power P_r , as a function of the imposed fault offset Δ and the angle Φ formed by the deformed pipe trunk with respect to the undeformed pipe axis. The white line denotes the values of Φ minimizing P_r . Note that, for $\Delta = 0$, minimization implies $P_r = 0$, as expected

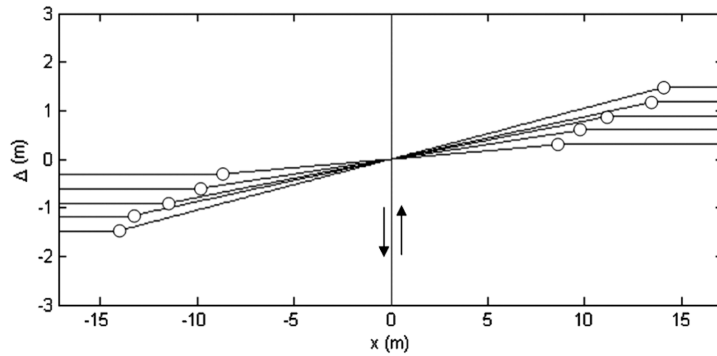


Fig. 4 Example of the failure mechanisms for different values of fault offset, in the case $\beta = 90^\circ$

3. Comparison with advanced 3D finite element simulations

3.1 Setup of the numerical model

To serve as an accurate benchmark to the previous simplified approach, a set of FE numerical simulations has been performed, where the response of soil and pipe steel, the soil-structure and the fault-structure interactions, and the kinematics of the pipe under large fault offset have been appropriately modeled. An updated Lagrangian formulation (Belytschko *et al.* 2000) has been adopted; the relevant implementation in the general-purpose FE code Abaqus was recently criticized in Ji *et al.* (2010), since it does not use fully work-conjugate stress and finite strain increments, and therefore overestimates the buckling loads of highly orthotropic, short structural members. In our study we instead focus on very slender pipes made of (isotropic) steel and, as mentioned in the Introduction, we are not aiming to capture very localized failure modes like wrinkling. Hence, the aforementioned drawbacks of the FE implementation do play a minor role in the results. In the FE simulations:

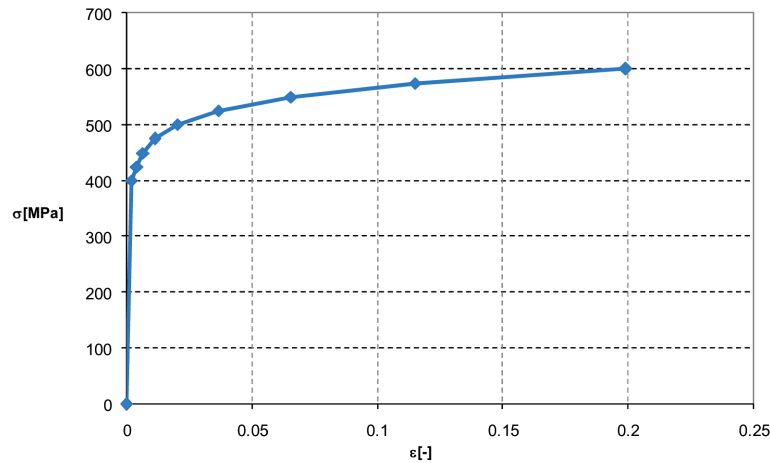


Fig. 5 Target uniaxial true stress vs logarithmic strain response of API X60 steel

- the behavior of the pipeline steel (API X60) has been modeled according to J_2 flow theory of plasticity (Simo and Hughes 1998), allowing for isotropic hardening; the relevant (target) uniaxial true stress vs logarithmic strain is illustrated in Fig. 5;
- yielding/failure of soil has been modeled through a perfectly-plastic Drucker-Prager criterion, allowing for non-associativity due to internal friction and compaction under highly compressive states of stress;
- the interaction between the outer surface of the buried pipeline and the surrounding soil, and between the two soil blocks along the strike-slip fault (whose orientation relative to the pipe longitudinal axis can be arbitrarily varied), has been assumed to be frictional. Allowing for potentially large displacement discontinuities, slip along the surfaces in contact locally occurs when $\tau_s > \mu\tau_n$, where τ_s and τ_n are the tangential and normal (compressive) components of the resolved traction field, respectively, and μ is the friction coefficient (either relevant to the soil-soil or to the pipe-soil interaction).

To avoid any spurious numerical disturbance caused by improper constraining of the pipeline, the size of the region surrounding the pipe and considered in the analyses have to lead to size-independent estimations of the load-carrying capacity of the pipe and of the local kinematics at failure. After a preliminary parametric investigation, we found that this is achieved if length L , width W and height H of the aforementioned region fulfill the constraints (Fig. 6): $L/D \geq 100$, $W/D \geq 30$, $H/D \geq 15$, and $H/Z \geq 8$, where $D = 2R_c$ and Z are the external cross-sectional diameter of the pipe and the burial depth of the pipe axis, respectively.

Assuming the slip along the fault to be governed by far-field loading, suitable displacement boundary conditions have been applied along the outer boundaries of the two soil blocks, as shown in Fig. 7. The pipeline was instead constrained at the cross-section ends along its longitudinal direction, so to account for the stiffening effects of the adjacent segments. Therefore, the pipe wall gets deformed only because of its interactions with fault and surrounding soil, according to what experienced by pipelines during fault slip.

Soil and pipe have been both meshed using 8-node brick elements. The characteristic size of the soil elements has been progressively decreased around the pipe (see Fig. 6), to improve accuracy in

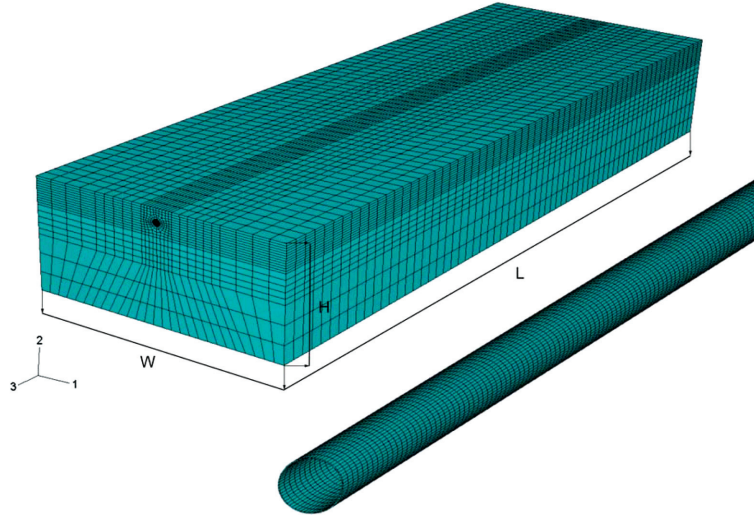


Fig. 6 Three-dimensional view of the modeled domain, showing the meaning of L , W and H and the typically adopted space discretization, with mesh refinement in the soil next to the pipe

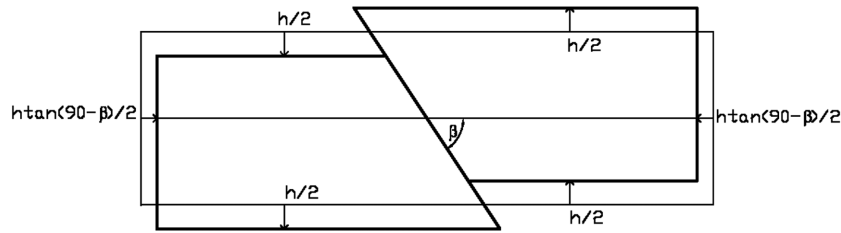


Fig. 7 Plan view of the boundary conditions adopted to induce fault slip and pipeline failure. $h/2$ denotes the imposed transverse displacement

the solution. Accuracy has not been detrimentally affected by having adopted brick elements to discretize also the pipe; in fact, local shell-like buckling deformation modes, as induced by fault slip, are captured by the adopted fine mesh (at least when compared to the characteristic size of the pipeline). This choice greatly simplifies the handling of the contact conditions between the outer surface of the pipe and the surrounding soil.

As far as loading condition is concerned, in a preliminary step only the weight of soil and pipeline have been accounted for, to define the state of stress prior to any fault slips. Having obtained this equilibrium state at-rest, the slip along the fault has been quasi-statically increased till the desired limit state is achieved. In this work, we have defined the allowable strain values for welded steel pipelines according to the Eurocode 8, Part 4 (CEN 2006), namely

- allowable tensile strain: 0.03 (13a)

- allowable compressive strain: $\min [0.01; 0.2 t/R_e]$ (13b)

where the latter values account for the reduced resistance in compression, due to local or global buckling.

3.2 Results of numerical simulations and comparisons with the proposed simplified approach

The 3D FE pipe model introduced previously is a useful tool to analyze the different stages of the strength mobilization, and allows one to recognize the most important factors affecting the pipe response to permanent ground displacements and its interaction with the surrounding soil.

The mesh consists of about $6 \cdot 10^4$ elements and $9 \cdot 10^4$ nodes. Each numerical simulation lasts about 23 h using 4 CPUs on a workstation with two quad-core Intel Xeon E5405 2.0 GHz processors, for a total CPU time of over 90 h. Parametric studies have been conducted based on a specific soil-structure model, with the main objective to compare FE results with those obtained by the simplified analytical method introduced in this paper, by considering the full range of possible values of the pipe-fault intersection angle (β), and to assess the performance of the pipe both under tensile ($0^\circ < \beta < 90^\circ$) and compressive ($90^\circ < \beta < 180^\circ$) deformations.

A X-60 steel pipeline has been considered (Fig. 5), with the following geometrical properties: $R_e = 0.305$ m (radius); $t = 9.5$ mm (thickness of the pipe cross-section); $Z = 1.215$ m (pipe axis burial depth). The modeled pipe length is $L = 60$ m (about 100 pipe diameter). As for the soil, the following parameters were considered: $\varphi = 30^\circ$ (shear resistance angle); $c = 10$ kPa (cohesion); $\gamma = 15$ kN/m³ (soil unit weight); $E = 5$ MPa (reduced soil elastic modulus). The pipe-soil friction angle ψ has been assumed equal to the soil shear resistance angle φ .

After the first step of the analysis, in which geostatic equilibrium is achieved, the fault displacement Δ has been gradually increased until the pipe reached the limit state condition described by Eqs. (13). An illustration of the onset of plastic deformations along the pipe for increasing values of Δ and $\beta = 80^\circ$ is shown in Fig. 8, while the same is shown in Fig. 9 for $\beta = 100^\circ$.

In the first case ($\beta < 90^\circ$), the mobilization of the pipe strength is governed by tensile deformation, mainly concentrated at the intersection of the pipe with the fault. In the second case ($\beta > 90^\circ$), the pipe response to fault offset at failure is governed by local compressive buckling: strains tend to concentrate at two cross-sections, anti-symmetric with respect to the fault trace, while the rest of the pipe tends to behave as a rigid body.

To verify the consistency of FE results with respect to the proposed simplified approach, we have first checked the values of the force resultant per unit length along the pipe-soil interface, along the longitudinal and transverse directions respectively, at the final step of the FE analysis. Denoting such values by t_{FE} and p_{FE} , respectively, these were compared with the limit unit force t_u and p_u , used in Eqs. (8) and (11), defined according to the empirical formulas available in the literature (see e.g. ALA 2001). For the case $\beta = 90^\circ$, it was found $t_{FE} = 17.2$ kN/m against $t_u = 20.1$ kN/m and $p_{FE} = 76.7$ kN/m against $p_u = 74.5$ kN/m in the part of the model where the failure condition is approached. Note however that a proper comparison is not possible since, while a limit value at failure is considered throughout the pipe length in the simplified approach, the FE analysis was stopped at the limit strain value defined by Eqs. (13), thus before attaining the complete mobilization of the plastic resources of the soil.

Considering now the comparison in terms of deformation levels, a synthesis of results of the parametric FE analysis is shown by the thick line in Fig. 10, where the fault offset Δ required to produce the limit state defined by Eqs. (13) is plotted as a function of β . The dramatic change of pipeline performance when moving from a tensile deformation style ($\beta < 90^\circ$) to a compressive one ($\beta > 90^\circ$) is clearly depicted, as the pipeline offset required to produce the prescribed limit state decreases by a factor of about 10.

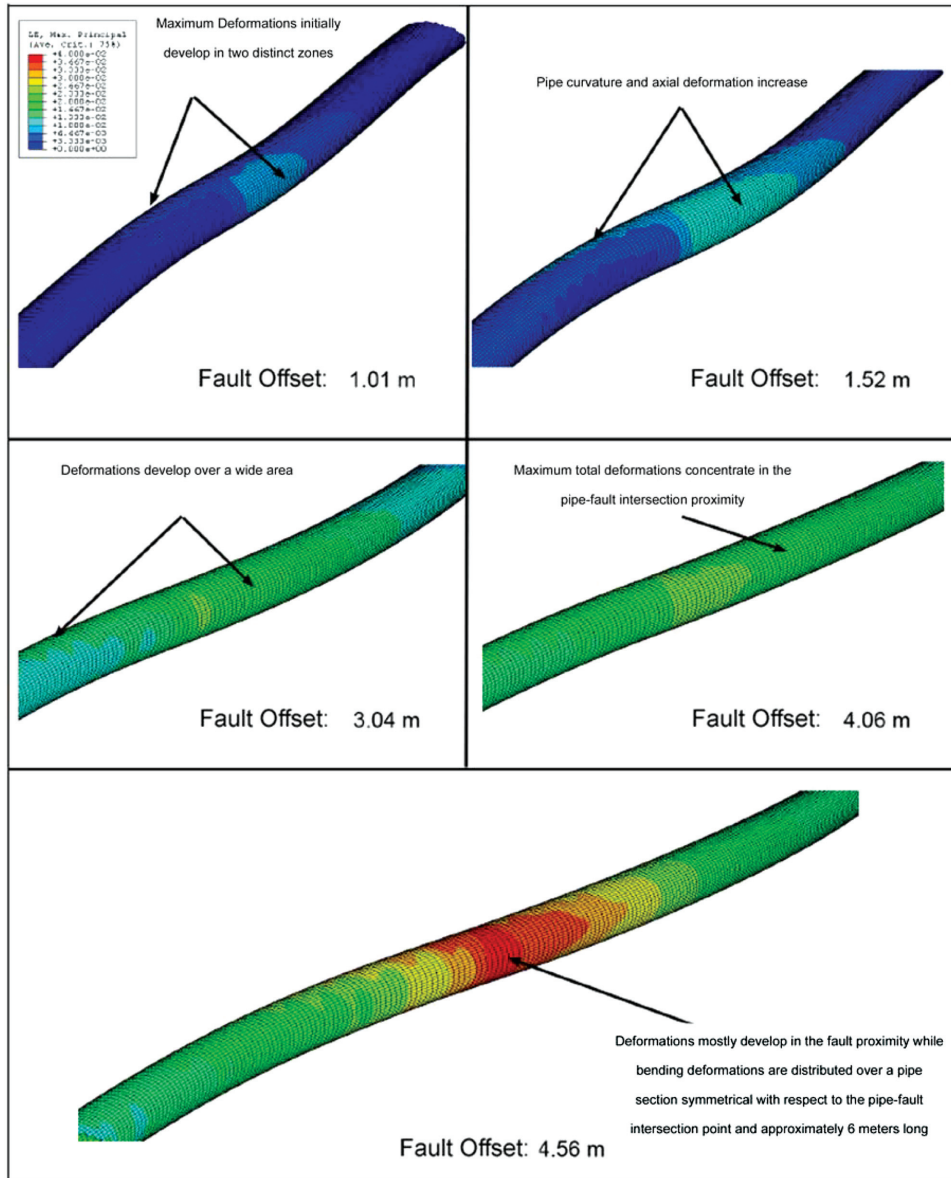


Fig. 8 Pipe behaviour for increasing values of the fault offset Δ for $\beta = 80^\circ$

In the same figure, results from two simplified approaches are also shown. Namely, the limit offset predicted according to the Kennedy *et al.* (1977) approach (thin dashed line) and the one predicted according to the simplified approach proposed in this paper (thin continuous line).

In the present simplified approach, the computed pipe strains refer to the plastic-hinge cross-sections, where the maximum values occur, while the other methods predict the maximum strain due to the elongation of the pipe at fault-crossing. The maximum pipe strain in the present approach is the sum of the flexural and elongation (axial) contributions. For the flexural contribution the strain is calculated as: $\varepsilon_f = \chi D/2$, where $\chi = \Phi/L_{ph}$ is the local pipe curvature and L_{ph} is the “length”

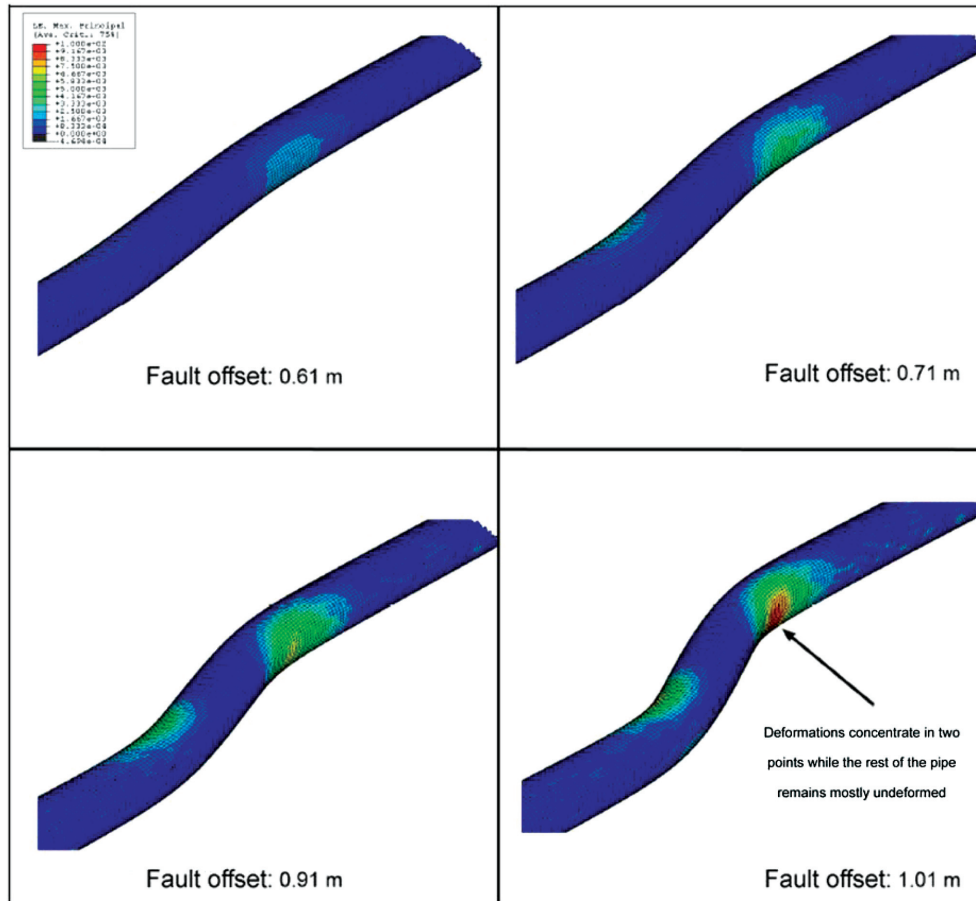


Fig. 9 Pipe behaviour for increasing values of the fault offset Δ for the case $\beta = 100^\circ$

of the plastic hinge. For thin-walled pipelines $L_{ph} = 2D$ can be tentatively used (Hoo Fatt and Xue 2001), so that

$$\varepsilon_f = \frac{\Phi}{4} \quad (14)$$

For the axial contribution, assumed to be constant along the pipe trunk between the two plastic hinges, simple geometrical relationships provide

$$\varepsilon_a = \frac{\sin\beta}{\sin(\beta - \Phi)} - 1 \quad (15)$$

Furthermore, in the simplified approach a value of the yield stress of the steel should be selected, according to a bi-linear stress-strain relationship, with no hardening. For a closer comparison with FE simulations, we have selected $\sigma_y = 515$ MPa, corresponding to $\varepsilon = 3\%$ in the uniaxial response of API X60 steel (Fig. 5).

As illustrated by Fig. 10, Kennedy's approach appears to be less conservative, as pointed out by previous works as well (e.g. Wong and Yeh 1985), mainly because of the cable-like assumption

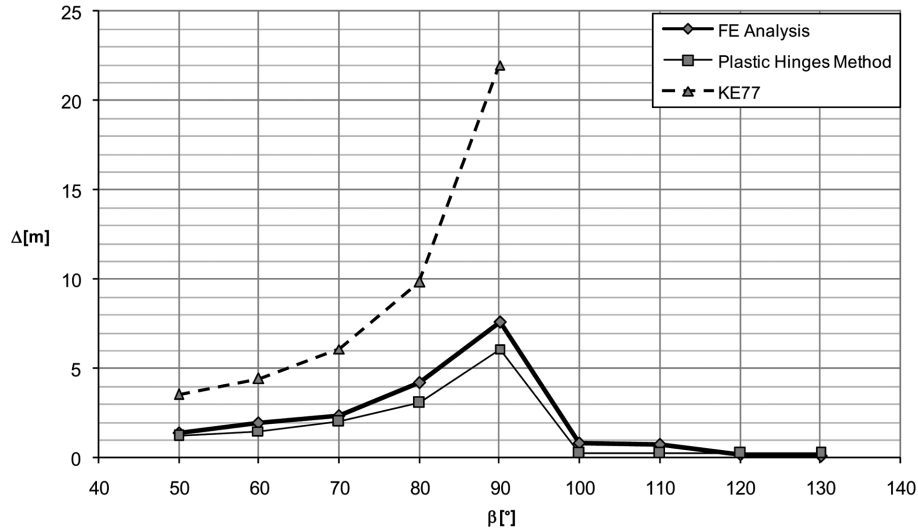


Fig. 10 Fault offset (Δ) required to produce the limit state defined by Eqs. (13) for the case under study. Dashed line: Kennedy *et al.* (1977) approach. Thick line: FE numerical simulations. Thin line: present simplified approach

about the pipe behaviour and because the two anchor points, based on which the elongation of the pipe is computed in Kennedy's method, turn out to be considered too far apart.

On the other side, the present simplified approach is more conservative than FE analyses. This can be explained, as in such simplified approach the axial strain is constant throughout the pipe trunk, so that the limit strain is always attained at the plastic hinges, where axial and flexural strains are superimposed. This is at variance with what observed from FE results, where it is clear that in the case $\beta < 90^\circ$ (see Fig. 8), the limit condition is attained due to the axial strain at the pipe-fault intersection.

In spite of this drawback, that highlights the limitation of this simplified approach to provide an accurate evaluation of the pipe behaviour at specific cross-sections, the global performance of the pipe is sufficiently well reproduced. Namely, it is important to note that the sharp reduction of the pipe strength for pipe-fault intersection angle $\beta > 90^\circ$ is well reproduced. It can be concluded that, while this approach is not in general suitable to predict the position of the most-critical cross-sections of the pipe, it can be effectively used for preliminary (and conservative) evaluations of the global performance of the pipe under a specific fault offset. Given the complexity of the numerical modelling of the problem, this can be considered as a satisfactory result.

4. Results of parametric analyses

Based on the satisfactory performance of the method to reproduce the global response of the buried pipeline under large strike-slip fault offsets, a set of parametric analyses has been carried out to check the relative influence of different parameters affecting the response of the pipe, namely: i) the angle β between the pipe axis and the fault surface trace; ii) the pipe-soil interface friction angle; iii) the embedment depth Z of the centre of the cross-section, normalized by its external diameter D ; iv) the cross-sectional thickness t , normalized by the external radius $R_e = D/2$. The

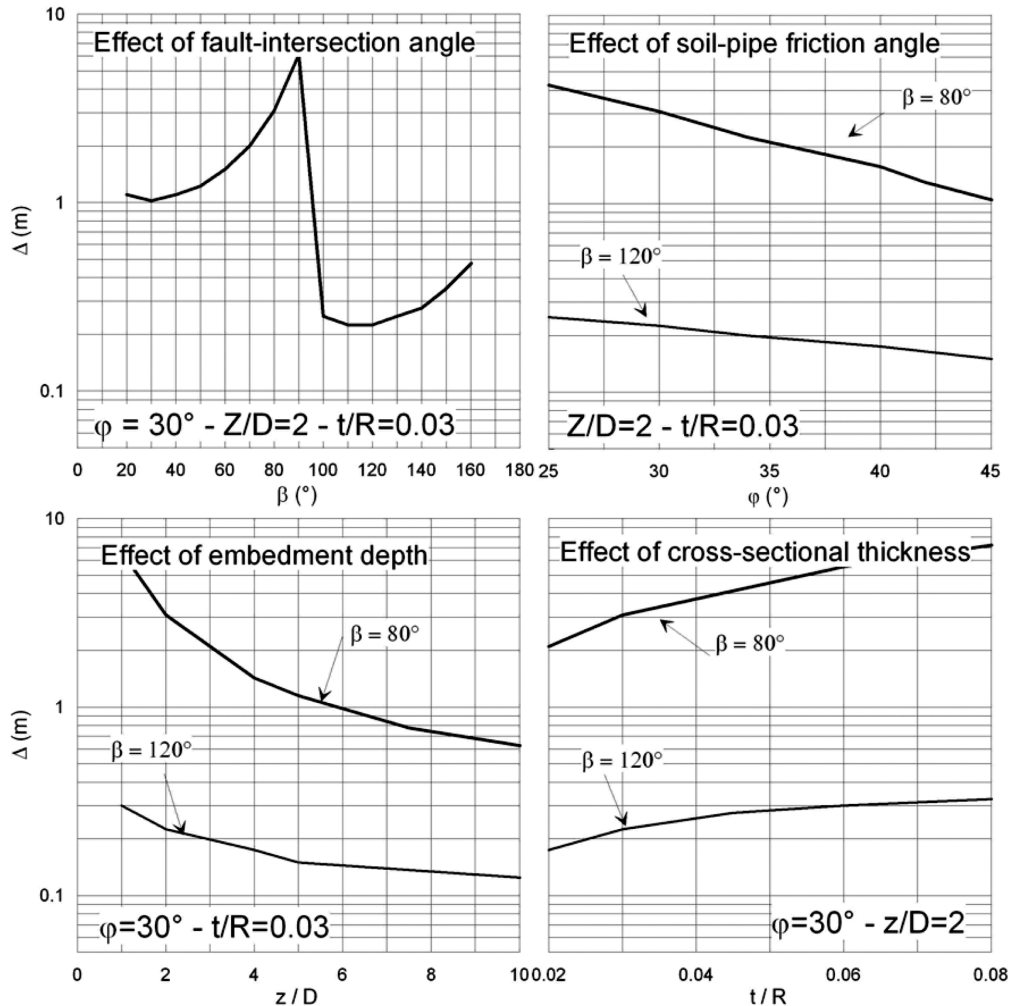


Fig. 11 Predicted fault offset Δ required to induce the allowable strain values (13), on a continuous pipeline subject to fault rupture. The parametric analysis shows results as a function of a) the angle β between the pipe axis and the fault surface trace, b) the pipe-soil interface friction angle, c) the embedment depth Z of the center of the cross-section, normalized by the external diameter D , d) the cross-sectional thickness t , normalized by the external radius $R_c = D/2$.

parametric analyses start from the same parameter set as selected for the previous comparison with FE simulations. The results of these analyses are plotted in Fig. 11, and show the predicted fault offset required to induce in the pipeline the allowable strain values defined by Eqs. (13).

All results plotted in Fig. 11 are in agreement, at least from a qualitative point of view, with the design measures suggested by the technical guidelines for buried pipelines at fault crossing (see, e.g. section 6.6 of Eurocode 8, Part 4), namely:

- the key role of the intersection angle of the pipe axis with respect to the fault trace to minimize compressive strains;
- the reduction of the angle of interface friction between pipe and soil, that improves the pipeline

behaviour since it induces the formation of plastic hinges far away from the fault intersection: in this way the flexural deformations are strongly reduced;

- the role of the embedment depth, coming implicitly into play in this approach by the expressions of t_u and p_u in Eqs. (8) and (11), respectively, that should be minimized in fault zones;
- the improved pipe behaviour for increasing cross-sectional thickness: it is to be noted that, according to the EC8 prescription, the allowable compressive strain is always attained due to the local buckling limit ($0.2 t/R_e$) for $t/R_e < 0.05$.

5. Conclusions

A method has been proposed for the simplified analysis of continuous pipelines intersecting a surface fault breakage. The method is based on the assumption that the failure mechanism consists of two plastic hinges on both sides of the pipe with respect to the fault, together with plastic elongation within the pipe trunk between the plastic hinges. The failure configuration is found by the minimization of the dissipated power, including the internal plastic dissipation in the pipe, together with the contributions of longitudinal and transverse sliding relative to the surrounding soil.

The method was shown to provide reasonable results, although more conservative than other simplified methods proposed in the past to solve the same problem: this can be easily explained since the previous methods do not allow for the reduction and loss of flexural cross-sectional stiffness as a consequence of large fault offsets. The reliability of the method has been confirmed by comparing results with an advanced 3D finite element approach, where the kinematics of the pipe and the soil under large deformations has been properly modeled.

As an example of application of the method, a set of plots has been produced showing the fault displacement required to produce the limit tensile or compressive strain according to Part 4 of Eurocode 8, as a function of different parameters such as the angle between the pipe axis and the fault surface trace, the soil-pipe interface friction angle, the embedment depth and the cross-sectional thickness.

In addition to its simplicity, the advantage of the proposed approach is that it can easily deal both with extensional and compressional deformation fields, and can be extended with no major difficulties both to normal and reverse faults. Furthermore, the proposed method can easily be extended to deal with inhomogeneous soil conditions, that may play an important role on the location of pipe damage. A potential further extension is the study of pipeline response to large landslide-induced offsets, for which failure mechanisms similar to those studied in this work can be proposed.

Acknowledgements

This work started when the first author was involved in the EC project QUAKER (“Fault-Rupture and Strong Shaking Effects on the Safety of Composite Foundations and Pipeline Systems”). The contributions of Anthony Le Caherec and Fabio Ratti in the initial phase is gratefully acknowledged. Daniela Pantosti has pointed out to the first author the case of the L'Aquila water transmission pipeline, examined within the EMERGEIO Working Group. Fruitful suggestions by two anonymous reviewers helped improving the paper.

References

- ALA (2001), *Guidelines for the design of buried steel pipes - Appendix B: Soil spring representation*, American Lifelines Alliance, <http://www.americanlifelinesalliance.org>.
- Belytschko, T., Liu, W.K. and Moran, B. (2000), *Nonlinear finite elements for continua and structures*, John Wiley & Sons, Ltd., Chichester, England.
- CEN (2006), *Eurocode 8 - Design of structures for earthquake resistance, Part 4: Silos, tanks and pipelines*, prEN 1998-4, Final draft, January 2006, Comité Européen de normalisation, Brussels.
- Eidinger, J.M., O'Rourke, M. and Bachhuber, J. (2002), "Performance of a pipeline at a fault crossing", *Proc 7th U.S. Nat. Conf. on Earthquake Engineering*, Oakland, California.
- Guo, E., Shao, G. and Liu, H. (2004), "Numerical study on damage to buried oil pipeline under large fault displacement", *Proc. 13th World Conf. on Earthq. Eng.*, Paper n. 2876, Vancouver, Canada.
- Ha, D., Abdoun, T.H., O'Rourke, M.J., Symans, M.D., O'Rourke, T.D., Palmer, M.C. and Stewart, H.E. (2008), "Centrifuge modeling of earthquake effects on buried high-density polyethylene (HDPE) pipelines crossing fault zones", *J. Geotech. Eng. - ASCE*, **134**(10), 1501-1515.
- Hoo Fatt, M.S. and Xue, J. (2001), "Propagating buckles in corroded pipelines", *Marine Struct.*, **14**(6), 571-592.
- Houliara, S. and Karamanos, S.A. (2006), "Buckling and post-buckling of long pressurized elastic thin-walled tubes under in-plane bending", *Int. J. Nonlinear Mech.*, **41**, 491-511.
- Ji, W., Waas, A.M. and Bazant, Z.P. (2010), "Errors caused by non-work-conjugate stress and strain measures and necessary corrections in finite element programs", *J. Appl. Mech. - ASME*, **77**, 044504-1-5.
- Kennedy, R.P., Chow, A.W. and Williamson, R.A. (1977), "Fault movement effects on buried oil pipeline", *J. Transp. Eng. Division - ASCE*, **103**(TE5), 617-633.
- Karamitros, D.K., Bouckovalas, G.D. and Kouretsis, G.P. (2007), "Stress analysis of buried steel pipelines at strike-slip fault crossings", *Soil Dyn. Earthq. Eng.*, **27**, 200-211.
- Liu, A., Takada, S. and Ho, Y. (2004), "A shell model with an equivalent boundary for buried pipelines under the fault movement", *Proc. 13th World Conf. on Earthq. Eng.*, Paper n. 613, Vancouver, Canada.
- Miyajima, M. and Hashimoto, T. (2001), "Damage to water supply system and surface rupture due to fault movement during the 1999 Ji-Ji earthquake in Taiwan", *Proc. 4th Int. Conf. Rec. Adv. in Geotechnical Earthq. Eng. and Soil Dyn.*, San Diego, CA, Paper 10.45.
- Newmark, N.M. and Hall, W.J. (1975), "Pipeline design to resist large fault displacement", *Proc. U.S. National Conference on Earthquake Engineering*, Ann Arbor, Michigan, 416-425.
- Ogawa, Y., Yanou, Y., Kawakami, M. and Kurakake, T. (2004), "Numerical study for rupture behavior of buried gas pipeline subjected to seismic fault displacement", *Proc. 13th World Conf. on Earthq. Eng.*, Paper n. 724, Vancouver, Canada.
- Oka, S. (1996), "Damage of gas facilities by Great Hanshin earthquake and restoration process", *Proc. 6th Japan-US Workshop on Earthquake Resistant Design of Lifeline Facilities and Countermeasures against Soil Liquefaction*, NCEER-96-0012, MCEER, Buffalo, NY, 111-124.
- O'Rourke, M.J. and Liu, X. (1999), *Response of buried pipelines subject to earthquake effects*, Multidisciplinary Center for Earthq. Eng. Research, Buffalo, NY, 249 pp.
- O'Rourke, M.J. and Deyoe, E. (2004), "Seismic damage to segmented buried pipe", *Earthq. Spectra*, **20**, 1167-1183.
- O'Rourke, T.D. and Palmer, M.C. (1996), "Earthquake performance of gas transmission pipelines", *Earthq. Spectra*, **12**, 493-527.
- Pineda-Porras, O.A. and Najafi, M. (2010), "Seismic damage estimation for buried pipelines - challenges after three decades of progress", *J. Pipeline-Syst.-Eng. Pract. - ASCE*, **1**, 1-19.
- Simo, J.C. and Hughes, T.J.R. (1998), *Computational Inelasticity*, Book Series: Interdisciplinary Applied Mathematics, Vol. 7, Springer New York.
- Takada, S., Hassani, N., Fukuda, K. (2001), "A new proposal for simplified design of buried steel pipes crossing active faults", *Earthq. Eng. Struct. Dyn.*, **30**, 1243-1257.
- Wang, L.R.L. and Yeh, Y. (1985), "A refined seismic analysis and design of buried pipeline for fault movement", *Earthq. Eng. Struct. Dyn.*, **13**, 75-96.